Science of Sintering, **52** (2020) 15-23

doi:https://doi.org/10.2298/SOS2001015S

UDK: 621.375.826; 669.018

The Effect of Synthesis of the Starting Powders on the Properties of Cu-Ti-TiB_2 Alloy Obtained by Laser Melting

J. Stašić*), D. Božić

Institute of Nuclear Sciences "Vinča", University of Belgrade, Mike Petrovića Alasa 12-14, PO Box 522, 11001 Belgrade, Serbia

Abstract:

A comparison was made between layer-by-layer laser melting (LM) of two types of feedstock powders: (1) elemental powder blend and (2) mechanically alloyed powder. LM was done by Nd:YAG laser at 1064 nm (max. average power 100 W) in argon ambience. Samples synthesized were Cu-Ti-TiB_2 rectangular tracks (20×6×1 mm), and input parameters of the process: powder layer thickness 100-250 μm, hatch spacing 1 mm, pulse length 4 ms, energy 4 J, pulse repetition rate 20 Hz. Part of the samples was heat-treated in argon at 900 °C, 10 h. Structural characterization of the samples was done using light microscope and scanning electron microscope (SEM). Chemical analysis of the as-obtained laser melted samples was done by inductively coupled plasma-atomic emission spectrometry (ICP-AES). It was established that the microstructure of LM samples was comprised of Cu-Ti and Cu-B solid regions, and in situ formed microparticles of primary TiB_2. Only after high-temperature thermal treatment has the secondary TiB_2 occurred. Tensile tests showed much higher strengthening in heat-treated samples with mechanically alloyed powder as starting material, where the formation of secondary TiB_2 nanoparticles was considerable.

Keywords*: Cu-Ti-TiB_2 alloy; Blending and mechanical alloying; Laser melting; Heat treatment; In situ TiB_2 reinforcements.*

1. Introduction

Laser melting (LM) is a unique additive manufacturing (AM) technology for production of complex-shaped objects with mechanical properties comparable to bulk material. Also, LM is one of few Rapid Prototyping (RP) techniques used for obtaining of composite materials [1-3]. SLM is controlled through set of parameters comprising process parameters [4], properties of powders subjected to radiation [5] and physico-chemical parameters of the process [6]. It is considered that the most important parameters in the process of laser melting are: laser power, scanning speed, hatch distance and layer thickness. These parameters were the ones mostly studied in the investigations related to this area. However, in order to obtain 3D compact of desired properties, numerous other parameters are not to be neglected. Aside from parameters related with laser and interaction process between laser beam and powder, there was a lot of research on parameters connected with starting material, i.e. their effect on microstructural, physical and mechanical characteristics of the final product. Particularly, the influence of shape [7] and size distribution [8] of the individual powder particles was studied, as well as the influence of powder tapped density and surface oxidation degree on the properties of LM compact [9]. Apart from these parameters, one of the important conditions for obtaining compacts with desired properties in metal alloys and

*) **Corresponding author:** jelsta@vinca.rs

composites is certainly preparation of powders for laser melting. Starting materials for production of 3D compacts by laser melting can be mixtures of elementary powders, prealloyed powders of the appropriate composition, or coated powders where particles of one metal are coated with particles of another metal [10]. All of these three ways have their advantages and disadvantages depending on the nature and composition of the constituents comprising alloy or composite. The advantage of using prealloyed powders is a homogeneous chemical composition of the material. The downside is a weaker control of the melting process due to dependence of the laser melting parameters (temperature, viscosity and surface tension) on the bulk composition. In mixed powders, a better control is achieved regarding viscosity and surface tension compared to prealloyed powders, however the wetting is poorer, as well as the kinetics of liquid phase spreading which is generally longer that the melt pool life time. Coated powders provide better bonding and higher absorption of laser energy. On the other hand, problem which can occur with these powders is a sublimation of impurities in the coating.

The aim here was to investigate the effect of the mixture of elementary powders, i.e. mechanically alloyed powders of the same composition, on the formation of TiB_2 reinforcements in copper matrix during the process of obtaining Cu-Ti-TiB_2 composite by laser melting. Copper is a material of choice when high thermal and electrical conductivity are required, and various copper-based composites are developed for improving its mechanical properties [11]. Composite Cu-Ti-TiB_2 was selected due to its potential, considering its properties [12], as well as future applications in military industry [13] and nuclear technique [14, 15]. This multiple (precipitation and dispersion) strengthened material is superior in structural stability to the precipitation hardenable alloys (such as Cu-Ti, Cu-Cr, Cu-Zr, etc.), because the second phase (TiB_2) has no tendency to dissolve at high temperatures [16], a characteristic of the precipitation hardenable alloys . Also, since the second phase is inert, it reduces electrical conductivity only to the extent that it reduces the cross-section of the material. Thus, electrical conductivities of the order of 80-95 % IACS can be achieved [17].

2. Materials and Experimental Procedures

Starting powders employed in experiments were: water atomized copper, titanium produced by hydride-dehydride processes (both size <63 μm, 99.5 % purity), and amorphous boron obtained by reduction of boron oxide (size <0.08 μm, 97 % purity). Feedstock powders used were: (1) elemental powder blend, and (2) mechanically alloyed (MA) powder, with the goal of comparing their behavior during SLM. In case of powder blend, the ratio was Cu-1Ti-0.35B (wt.%) and homogenization was done for 1 h. The second powder was obtained by mixing for 1 h binary powders Cu-2wt%Ti and Cu-0.7wt%B which were first separately mechanically alloyed for 24 h. MA was done in argon using steel balls (diameter 6 mm), with ball/powder ratio 5:1 and stirring speed 330 rpm. Experiments were done in argon ambient, and rectangular samples of Cu-Ti-TiB_2 (20×6×1 mm) were obtained in layer-by-layer manner using Nd:YAG millisecond laser. Process parameters employed were as follows: pulse repetition rate 20 Hz, pulse duration 4 ms, energy ~4 J, hatch distance 1 mm, and layer thickness ~100 μm/250 μm for mixed/MA powders. Some picese were thermally treated at 900 °C for 10 h in Ar. Chemical analysis of the as-obtained laser melted samples was done using inductively coupled plasma-atomic emission spectrometry (ICP-AES). Concentration of TiB_2 compound was determined from the internal standards formed for the referent samples of this compound.

Microstructure of the starting powders and LM samples was investigated by optical microscope (OM), as well as scanning electron microscope (SEM) connected with energy dispersive x-ray spectroscope (EDS). Metallographic preparation for OM comprised grinding,

polishing and etching in KLEM III solution (40 g K_2S, 11 ml $N_2S_2O_3$ and 100 ml H_2O). Density of the obtained samples was measured by Archimedes method in water. Ultimate tensile strength and elongation to fracture were tested on Instron universal testing machine (crosshead speed 0.5 mm/min, room temperature). Fractured surfaces were also observed with OM and SEM.

3. Results and Discussion

Morphology of the mixed powder for LM is shown in Fig. 1. The majority of Cu particles have irregular shape with the presence of some smaller rounded particles. Titanium particles were also irregularly shaped with sharp edges. It can be seen that the particles of alloying elements were uniformly distributed around the base Cu particles, i.e. the mixture was dominantly homogeneous which is critical for uniform absorptance of laser beam and melting. However, some agglomerations consisting of small particles can be clearly observed in given images. EDS analysis showed the presence of certain, not significant amount of oxygen on the surface of copper and titanium particles.

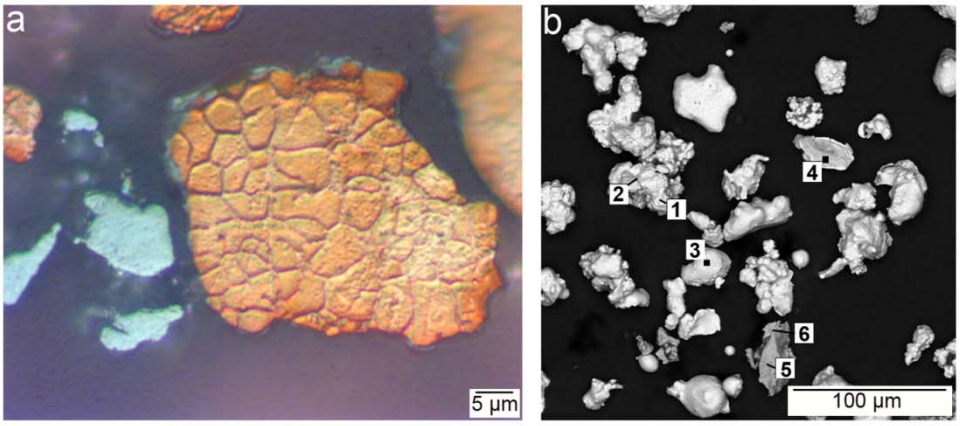

	Cu	Ti	B	O	Total
Spectrum 1	99.8			0.2	100.0
Spectrum 2	74.2		25.6	0.2	100.0
Spectrum 3	99.8			0.2	100.0
Spectrum 4		99.9		0.1	100.0
Spectrum 5		99.8		0.2	100.0
Spectrum 6		53.6	46.3	0.1	100.0

Fig. 1. Homogenized mixture of powders Cu-1Ti-0.35B (wt.%): a) OM; b) SEM.

Fig. 2 shows mechanically alloyed Cu-Ti, i.e. Cu-B powders (MA duration 24 h), with characteristic layers formed due to deformation, fracturing and welding of soft particles [18] leading to their microforging (Fig. 2a, b). Chosen milling parameters enabled alloying of copper particles with titanium and boron to a significant degree, which was confirmed with SEM images (Fig. 2c, d) and EDS quantitative analysis. The presence of boron could be identified only at higher magnification. Compared to mixed powders, number of agglomerated boron particles in mechanically alloyed Cu-B particles was lower.

Through LM process Cu-Ti-TiB_2 3D samples (~15 layers) were obtained, Fig. 3. Laser melting process was conducted so that in both cases (mixed and mechanically alloyed powders) building parameters of synthesis, as well as the content of alloying elements was the same.

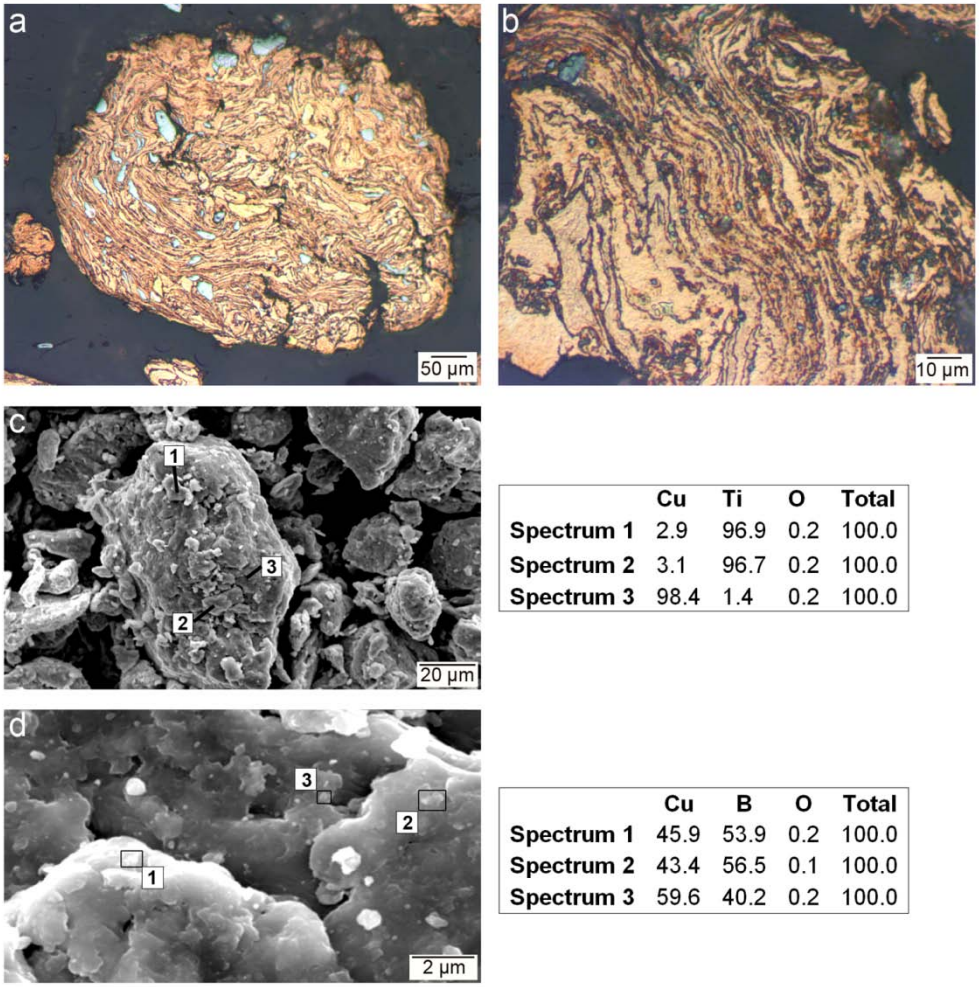

	Cu	Ti	O	Total
Spectrum 1	2.9	96.9	0.2	100.0
Spectrum 2	3.1	96.7	0.2	100.0
Spectrum 3	98.4	1.4	0.2	100.0

	Cu	B	O	Total
Spectrum 1	45.9	53.9	0.2	100.0
Spectrum 2	43.4	56.5	0.1	100.0
Spectrum 3	59.6	40.2	0.2	100.0

Fig. 2. Mechanical alloyed powders: microstructures of a) Cu-Ti particles; b) Cu-B particles ; morphology and EDS analysis of c) Cu-Ti particles; d) Cu-B particles.

Fig. 3. SLM part of Cu-Ti-TiB_2 alloy from mechanically alloyed powder, obtained under process parameters of 20 Hz; 4 ms; 4 mJ.

The overall porosity in laser melted samples from mixed powder was about 15 %. Due to *in situ* formation of TiB_2 particles and their rapid growth surface of the formed layer had prominent roughness, which led to a lot of empty space between melted layers, Figs. 4a and 4b. In laser melted samples with mechanically alloyed powder, Figs. 4c and 4d, there was not enough time for larger number of primary TiB_2 particles to form, nor for higher degree of

their coarsening. Particles were mostly formed on solid region boundaries. For that reason, melted layers were flatter and the overall porosity was lower, around 8 %.

Temperatures during interaction of laser beam with powder particles of copper alloys under these experimental conditions can reach 4000-5000 K, which enables formation of TiB_2 dispersoids by rapid solidification from these temperatures [19]. In compacts where the starting material was comprised of blended powders, preferential locations for formation of these ceramic particles were between base metal particles, although they could be formed also on the starting titanium particles. It can be noted from Figs. 4a and 4b that considerably large (even up to 10 μm) TiB_2 particles were formed. Formation of ceramic particles this big in the course of laser melting, as well as their wider size distribution, is characteristic for *in situ* obtaining of TiB_2 in liquid phase [20]. Most frequent locations for the formation of primary TiB_2 particles in compacts where the starting material were mechanically alloyed powders, were borders between Cu-Ti and Cu-B solid regions, where alloying elements are closest to one another. Formed TiB_2 particles were significantly smaller (submicron size and somewhat above 1 μm, Fig. 4c and 4d) than in previous case, due to longer diffusion paths titanium and boron atoms had to pass in order to form diborides.

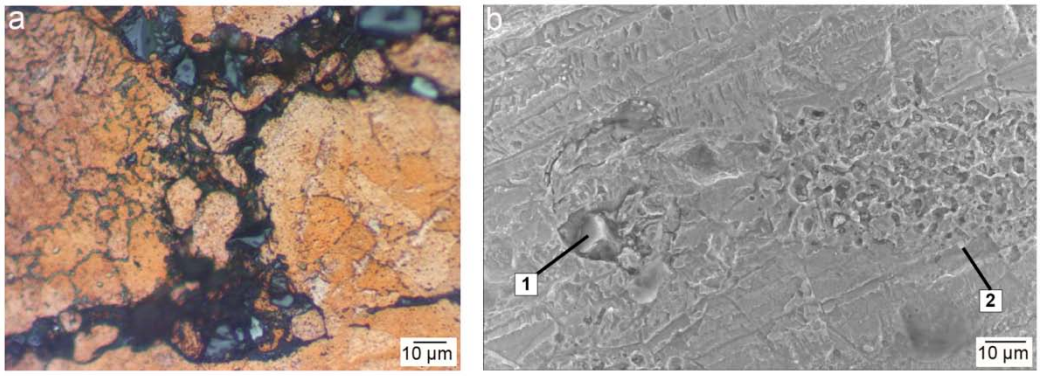

	Cu	Ti	B	O	Total
Spectrum 1	1.7	52.2	46.0	0.1	100.0
Spectrum 2	4.1	47.5	48.2	0.2	100.0

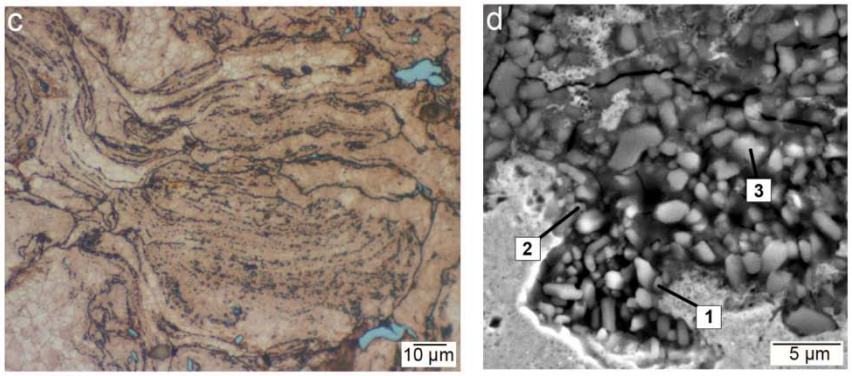

	Cu	Ti	B	O	Total
Spectrum 1	5.0	48.5	46.3	0.2	100.0
Spectrum 2	7.2	52.6	40.1	0.1	100.0
Spectrum 3	73.1	26.7		0.2	100.0

Fig. 4. Microstructure of Cu-Ti-TiB_2 samples produced by SLM of: a, b) blended powders; c, d) mechanical alloyed powders.

Fig. 5 shows UTS values for Cu-Ti-TiB_2 3D compacts obtained by laser melting of blended, i.e. mechanically alloyed powders. Values refer to the samples tested before and after appropriate heat treatment.

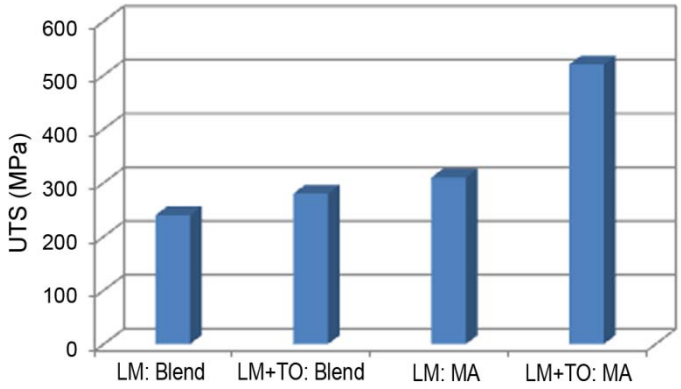

Fig. 5. UTS values of Cu-Ti-TiB_2 laser melted samples before and after heat treatment. Elongations were 1.5-6 %.

Obtained tensile strength values in both laser melted samples were low, which was expected due to significant presence of pores and cracks. Based on pore shape, conclusion regarding their origin could be made. Most common reasons for the formation of pores in the structure were weaker chemical bond, especially larger, TiB_2 particles and copper matrix, their falling out during preparation of samples for tensile tests (irregular pore shape, Fig. 4a, b) and vaporization of the base metal during laser melting (spherical pore shape, Fig. 4b). Residual stresses characteristics for laser melting process (rapid heating and cooling cycles) are the cause for the occurrence of cracks in the structure of these samples (Fig. 4d). Of course, the number of present microstructural defects could be lowered or completely eliminated through appropriate treatments prior to and after laser melting (e.g. by substrate heating before laser melting process or sintering under pressure to reduce or eliminate porosity). Optimization of the process parameters was not priority in this work, but the focus was on the formation of primary and secondary TiB_2 particles and exclusively their influence on the tensile properties of Cu-Ti-TiB_2 alloy. Somewhat higher UTS value in laser melted sample with mechanically alloyed powder is a consequence of better density and the presence of smaller number of coarser primary TiB_2 particles. By heat treatment at 900 °C, 10 h, we wanted to initiate the formation of secondary TiB_2 nanoparticles. Chosen heat treatment conditions were, according to literature [21], optimum for the formation of secondary TiB_2 particles. We noticed subtle reduction of porosity in both samples (from 15 to 12 % in samples with blended powder, i.e. from 8 to 6 % in samples with mechanically alloyed powder). Still high pore content and large number of coarse primary formed TiB_2 particles did not allow for a more significant increase in UTS, as well as ductility (from 1.5 to 2 %) in heat treated samples where blended powder was used as a starting material. The discussion was supported by fractographic and chemical analysis. Fig. 6 shows longitudinal and transversal section of the fracture in laser melted samples after the heat treatment. In both longitudinal (crack propagation direction, Fig. 6a) and transversal section (fracture surface, Fig. 6b) of the fracture in the laser melted samples where blended powder was a starting material , large TiB_2 particles could be observed as a preferential spot for the formation and propagation of cracks. The obtained value for UTS was an indicator that there were very few free Ti and B atoms in this sample for the formation of secondary TiB_2 particles. This was also confirmed

by chemical analysis (Tab. I), which shows almost unchanged content of TiB_2 particles before and after the heat treatment.

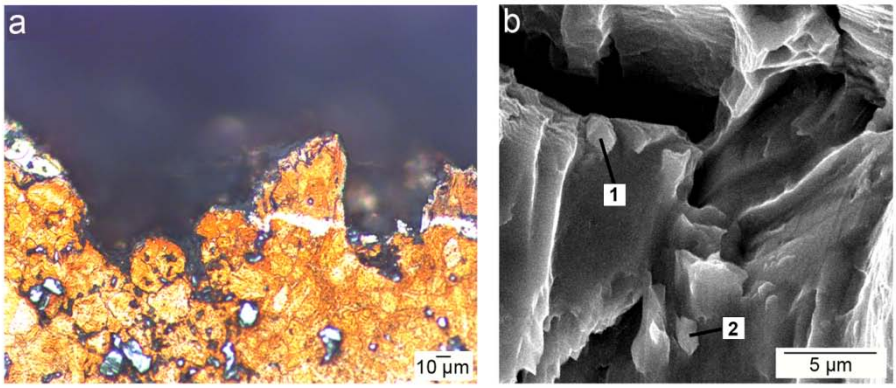

	Cu	Ti	B	O	Total
Spectrum 1	2.6	60.5	36.7	0.2	100.0
Spectrum 2	3.1	56.3	40.4	0.2	100.0

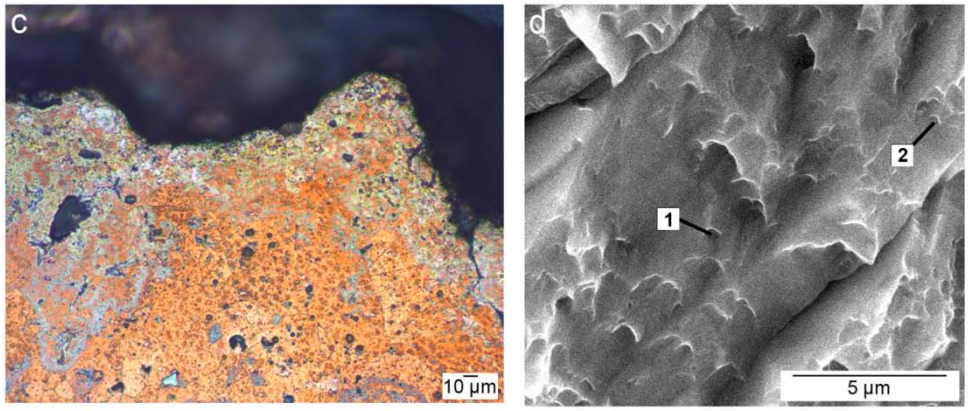

	Cu	Ti	B	O	Total
Spectrum 1	7.5	62.3	30.1	0.1	100.0
Spectrum 2	6.7	57.1	36.0	0.2	100.0

Fig. 6. Longitudinal (a, c) and transversal (b, d) section of the fracture in laser melted Cu-Ti-TiB_2 samples after the heat treatment.

Tab. I. Chemical analysis of the laser melted samples prior and after thermal treatment at 900 °C, for 10 h.

Starting powder	**SLM prior HT**	**SLM after HT**
Blended	Cu-0.3Ti-0.1B-0.85TiB_2(wt.%)	Cu-0.2Ti-0.05B-1.0TiB_2(wt.%)
Mechanically alloyed	Cu-0.75Ti-0.2B-0.3TiB_2(wt.%)	Cu-0.19Ti-0.01B-1.05TiB_2(wt.%)

In Fig. 6c, showing the direction of crack propagation, the presence of secondary crack is also observed, which implies better fracture resistivity of the tested sample compared to the sample from the blended powder. In relation to samples from blended powders with prominently brittle fracture surfaces, in samples from mechanically alloyed powders fracture surfaces showed the presence of ductile areas with characteristics dimples in certain parts of

the structure (Fig. 6 d). On the fracture surface, in higher magnification, submicron, primary TiB_2 particles could be identified.

After the heat treatment of the samples obtained from mechanically alloyed powder, tensile test showed completely different result, Fig. 5. Increase in the UTS was almost 70 %, while the ductility increased from 3 to 6 %. UTS value is most probably due to occurrence of secondary TiB_2 particles resulting from the reaction between Cu_4Ti and B [22]. These particles represent obstacles to the movement of dislocations in the compact, and their higher content in matrix brings a noTab. strength increase. Another factor that should be taken into account is the relaxation of residual stresses present in the SLM part through heating and retaining at 900 °C, which also has a positive effect on the UTS value. Of course, formed nanoparticles of secondary TiB_2 phase could not be observed by optical and scanning electron microscope, Fig. 4, but their presence was identified with chemical (Tab. I) analysis. ICP-AES analysis has shown considerbly higher content of TiB_2 phase particles after the heat treatment than prior to exposure to temperature of 900 °C for 10 h of the SLM compacts from mechanically alloyed powders.

4. Conclusion

Synthesis of Cu-Ti-TiB_2 alloy was conducted through laser melting of (i) blended Cu, Ti and B powders, i.e. (ii) mixed mechanically alloyed Cu-Ti and Cu-B powders. Microstructure of the obtained pieces contained solid regions Cu-Ti and Cu-B, with microparticles of primary TiB_2 formed *in situ*. It was necessary to conduct a thermal treatment (900 °C, 10 h) for the occurrence of secondary, nanoparticles of TiB_2, which was detected using ICP-AES analysis and tensile testing of 3D parts. Tensile tests have shown that the strengthening was much higher in heat-treated samples with mechanically alloyed powder as the starting material, due to a more significant formation of secondary TiB_2 nanoparticles.

Acknowledgments

The results presented are realized with a financial support of the Ministry of Education, Science and Technological Development of the Republic of Serbia through project no. 172005.

5. References

1. G. Levy, R. Schindel, J.P. Kruth, Ann. CIRP, 52 (2003) 589.
2. D.T. Pham, S.S. Dimov, C. Ji, R.S. Gault, in: Proc. 1st International Conference on Advanced Research in Virtual and Rapid Prototyping, Portugal, 2003, p. 107-113.
3. S. Kumar, J.P. Kruth, Mater. Des., 31 (2010) 850.
4. J.A. Cherry , H.M. Davies , S. Mehmood , N.P. Lavery , S.G.R. Brown, J. Sienz, Int. J. Adv. Manuf. Technol., 76 (2015) 869.
5. M. Rombouts, Selective laser sintering/melting of iron-based powders, Ph.D. thesis, Katholieke Universiteit Leuven, 2006.
6. J.P. Kruth, M. Badrossamay, E. Yasa, J. Deckers, L. Thijs, J. Van Humbeeck J, in: Proc. 16th International Symposium on Electromachining (ISEM XVI), Shanghai, China, Shanghai Jiao Tong University Press, Shanghai, 2010, p. 1-12.
7. N. Nomura, K. Kikuchi, A. Kawasaki, in: Proc. World PM2016 congress, Hamburg, 2016.

8. J. Dawes, R. Bowerman, R. Trepleton, Johnson Matthey Technol. Rev., 59 (2015) 243.
9. T. Talako, A. Letsko, J. Miner. Met. Mater. Eng., 3 (2017) 95.
10. D.C. Walker, W.F. Caley, M. Brochu, J. Mater. Res., 29 (2014) 1997.
11. M. Darabi, M. Rajabi, B. Junipour, M.T. Noghani, Sci. Sint. 50 (2018) 477.
12. D. Bozic, I. Cvijovic-Alagic, B. Dimcic, J. Stasic, V. Rajkovic, Sci. Sint., 41 (2009) 143.
13. H.H. Liebermann, N.J. Grant, T. Ando, Selected examples of application, in: Elements of rapid solidification: Fundamentals and Applications, Ed. M.A. Otooni, Springer, Berlin, 1998. p. 217-236.
14. M.G. Kalinin, A.S. Fabritsiev, N.B. Singh, S. Tahtinen, J.S. Zinkle, J. Nucl. Mater. 307-311 (2002) 668.
15. M. Li, S.J. Zinkle, Compr. Nucl. Mater. 4 (2012) 667.
16. M. Vlasova, A. Bykov, M. Kakazey, P.A. Marquez Aguilar, I. Melnikov, I. Rosales, R. Guardian Tapia, Sci. Sint. 48 (2016) 137.
17. J. Ružić, J. Stašić, V. Rajković, D. Božić, Mater. Des. 49 (2013) 746.
18. V. Rajković, O. Erić, D. Božić, M. Mitkov, E. Romhanji, Sci. Sint. 36 (2004) 205.
19. J. Stasic, D. Bozic, J. Alloy Comp., 762 (2018) 231.
20. A. Chrysanthou, G. Erbaccio, J. Mater Sci., 30 (1995) 6339.
21. M. Sobhani, H. Arabi, A.R. Mirhabibi, JNS, 2 (2013) 519.
22. S.J. Dong, Y. Zhou, Y.W. Shi, B.H. Chang, Metall. Mater. Trans. A 33A (2002) 1275.

Сажетак: *У раду је извршено поређење ласерског топљења (ЛТ) техником слој-по-слој за две врсте почетног праха: (1) мешавину елементарних прахова и (2) механички легиран прах. Ласерско топљење вршено је Nd:YAG ласером на 1064 (максималне средње снаге 100 W) у атмосфери аргона. Синтетизовани узорци су били Cu-Ti-TiB_2 правоугаоне траке (20×6×1 mm),а улазни параметри процеса: дебљина слоја праха 100-250 μm, размак између скенирајућих редова 1 mm, дужина импулса 4 ms, енергија 4 J, учестаност импулса 20 Hz. Део узорака је термички третиран у аргону на 900 °C, 10 h. Структурна карактеризација узорака вршена је коришћењем оптичког микроскопа и сканирајућег електронског микроскопа (СЕМ). Хемијска анализа узорака добијених ласерским топљењем урађена је помоћу технике атомске емисионе спектрометрије путем индуктивно спрегнуте плазме (ICP-AES). Утврђено је да се микроструктура ЛТ узорака састоји од Cu-Ti и Cu-B чврстих области, и in situ формираних микрочестица примарног TiB_2. Тек након високотемпературског термичког третмана дошло је до формирања секундарног TiB_2. Затезна испитивања показала су знатно веће очвршћавање код термички третираних узорака са механички легираним прахом као почетним материјалом, где је дошло до формирања значајне количине секундарних наночестица TiB_2.*

Кључне речи*: Cu-Ti-TiB_2 легура; мешање и механичко легирање; ласерско топљење; термички третман; in situ TiB_2 ојачивачи.*